Dyes and Pigments 92 (2011) 659–667

Contents lists available at ScienceDirect

Dyes and Pigments

journal homepage: www.elsevier.com/locate/dyepig

# Synthesis and characterization of a range of POSS imides

David Clarke [a,*], Simon Mathew [b], Janis Matisons [c], George Simon [d], Brian W. Skelton [e]

[a] School of Chemical & Physical Sciences, Flinders University, Bedford Park, 5042 South Australia, Australia
[b] Department of Molecular Engineering, Graduate School of Engineering, Kyoto University, Nishikyo-ku, Kyoto 615-8510, Japan
[c] Gelest Inc., 11a Steel Road, Morrisville, PA 19067, USA
[d] Department of Materials Engineering, Monash University, Clayton, 3800 Victoria, Australia
[e] School of Biomedical, Biomolecular and Chemical Sciences, University of Western Australia, Crawley, Perth, Western Australia 6009, Australia

ARTICLE INFO

*Article history:*
Received 29 March 2011
Received in revised form
30 May 2011
Accepted 31 May 2011
Available online 15 June 2011

*Keywords:*
Silsesquioxane
Perylene
Naphthalene
Polyhedral oligomeric silsesquioxane
Rylene
Imide

ABSTRACT

The microwave condensation of mono-amino functionalised polyhedral oligomeric silsesquioxane (POSS) with a range of mono- and bis-anhydrides yielded the corresponding POSS imide compounds, which were characterized by UV–Vis and fluorescence spectrophotometry. The perylene POSS imide derivative was further characterized by single crystal X-ray crystallography. The naphthyl POSS bis/monoimide exhibited extremely weak fluorescence, whilst the perylene POSS bis-imide displayed particularly strong fluorescence, with a quantum yield approaching unity.



## 1. Introduction

Rylenes are hydrocarbon families, which can be regarded as naphthalene oligomers containing bonds between the 1 and 1′ positions and the 8 and 8′ positions of adjacent naphthalene units. Observations of electron transport behaviour and tunable molecular electronic properties, through N-substituent variation or rylene backbone manipulation motivated interest into rylene and diimides [1]. Rylene diimides exhibit relatively high electron affinities, high electron mobilities, and excellent chemical, thermal, and photochemical stabilities. Therefore, rylene diimides and their derivatives have found use in a variety of applications, such as organic light-emitting diodes [2], dye lasers [3], optical switches [4], and photodetectors [5], and also as electron acceptors for studying photoinduced energy and electron-transfer processes [6–8].

Perylenes have been used in electronic applications where they are among the best available *n*-type semiconductors [9,10]. The *n*-type semi-conductivity is related to the high electron affinity of the rylene bis-imide dyes [11], making the perylene bis-imide family promising for use as organic field transistors [12]. Perylene bis-imides also possess a unique combination of optical, redox and stability properties, which have led to them being investigated in electrophotography [5], pH sensing [13], and photovoltaics [14,15]. However, a significant drawback of perylene dyes is the tendency for formation of dye aggregates through extended $\pi$-systems [16,17].

Another class of widely exploited imides, phthalic diimides are relatively transparent to visible light compared to naphthalene or perylene tetracarboxylic diimides with the same side chain, due to the reduced $\pi$-conjugation length. This has led to them being investigated as promising candidates for transparent electronics [18].

POSS based hybrid materials have recently emerged as unique materials due to their enhanced physical and mechanical properties, compared to the parent polymer. Properties such as temperature and oxidation resistance, surface hardening, mechanical properties, reduced flammability and diminished exothermicity on combustion are improved through the covalent linkage of POSS within the polymer matrix [19–22]. The suppression of such aggregation in conjugated chromophores and polymers, featuring aromatic systems such as carbazole, terfluorene [23] and polyfluorene through the incorporation of POSS cages has been previously reported [23–28].

POSS offers an ideal core to introduce multifunctionality, specifically octa- and tri-functionalised molecules. As a result, the study of the synthesis and properties of a variety of functionalised POSS mono- and diimide adducts were of interest in the pursuit of

* Corresponding author. PO Box 31-310, Lower Hutt 5040, New Zealand. Tel.: +64 49313240; fax: +64 49313306.
*E-mail address:* d.clarke@irl.cri.nz (D. Clarke).

0143-7208/$ – see front matter © 2011 Elsevier Ltd. All rights reserved.
doi:10.1016/j.dyepig.2011.05.028

developing multifunctional high performance optical materials. Mono-functionalised POSS compounds were employed in order to provide a useful starting point for the investigation into the synthesis and properties of POSS imides. Microwave synthesis was employed in order to provide a facile synthetic pathway to mono-functionalised POSS mono- and diimides.

## 2. Experimental

### 2.1. Instrumentation

$^{1}H$, $^{13}C$ and $^{29}Si$ NMR were recorded on a 300 MHz Varian Gemini FT-NMR. Chemical shifts ($\delta$) are reported in parts per million (ppm), with solvent peaks used as references for $^{1}H$ and $^{13}C$ NMR spectra. External tetramethysilane was used as a reference for $^{29}Si$ NMR spectra. FTIR spectra were obtained on a Nicolet Nexus 8700 FTIR spectrometer and data analysis was performed using Omnic 7.0 software. A Diffuse Reflectance Infra Red Transmission (DRIFT) spectroscopy accessory was used in combination with the FTIR for solid sample analysis. Accurate mass ElectroSpray Ionisation (ESI) analysis was performed on a Bruker BioApex II 47e Fourier Transform Mass Spectrometer (FT-MS), using Xmass Version 5.0 software at Monash University. Elemental analyses samples were submitted to the analytical department of the University of Otago, New Zealand, for analysis of carbon, hydrogen and nitrogen contents. UV–Vis experiments were performed at an ambient temperature of 25 °C using a Varian Cary 50 Scan Spectrophotometer. Steady-State Fluorescence experiments were conducted on a Varian Cary Eclipse Fluorescence Spectrophotometer equipped with a Varian single cell Peltier accessory used in conjunction with a Gilson MINIPULS3 peristaltic pump to aid temperature control of the sample.

### 2.2. Chemicals

Commercially available chemicals were used without purification unless otherwise stated. *i*-$Bu_7Si_7O_9(OH)_3$ was purchased from Hybrid Plastics (Hattiesburg, MS). The remaining chemicals were obtained from Sigma–Aldrich. Solvents were purified and dried according to literature procedures [29]. Mono-(3-aminopropyl) hepta-(*iso*-butyl) POSS was synthesised according to the previously reported procedure [30].

### 2.3. General synthetic procedure of POSS imides

The reactions of a variety of mono- and bis-anhydrides with mono-(3-aminopropyl) hepta-(*iso*-butyl) POSS (hereafter referred to as mono-amino POSS) are discussed herein. The condensation of the desired anhydrides with a large stoichiometric excess (approximately 4 fold) of mono-amino POSS was performed with the use of microwave radiation [31,32], with imidazole utilized as the solvent [33]. Microwave experiments were performed in a domestic microwave oven, modified for chemical use, similar to that detailed in the literature [34]. Thermal condensation of amino POSS with a range of mono- and bis-anhydrides has recently been reported [35,36], [20,37] however the use of microwave radiation enabled the synthesis of the desired POSS imides to occur in a greatly reduced timeframe. Thermal methods involved reaction times ranging from 4 to 24 hr at elevated temperatures, which were reduced to 5 min with the use of microwave radiation. Purification was achieved by washing with dilute hydrochloric acid and water, followed by column chromatography (eluant hexane/chloroform), to yield the desired POSS imide.

#### 2.3.1. Mono-phthalic POSS imide (**2a**)

All POSS mono- and diimides were synthesised according to the method for the mono-phthalic POSS imide (**2a**) outlined below. Phthalic anhydride (166 mg, 1.12 mmol), mono-(3-aminopropyl) hepta-(*iso*-butyl) POSS (3.918 g, 4.48 mmol, 4 equiv.) and imidazole (12.2 g, 17.9 mmol, 16 equiv.) were combined. The mixture was reacted in a modified microwave reactor for approximately 5 min, with homogenisation performed as required (typically, every 30 s) [31]. Tetrahydrofuran (100 mL) and hydrochloric acid (100 mL, 3 M)

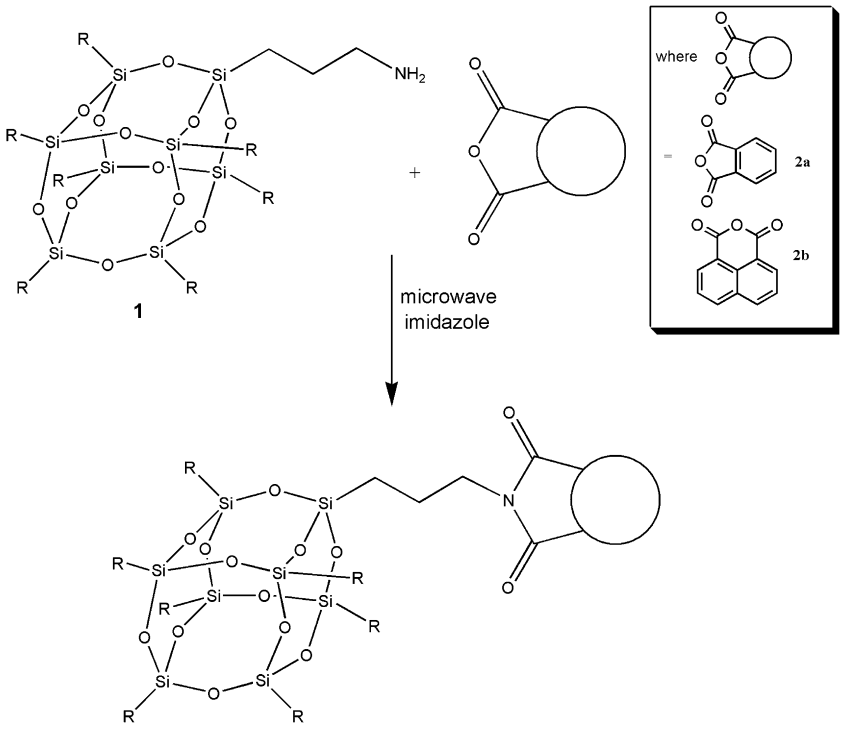


**Fig. 1.** Synthesis of POSS mono-imides.

were added and the solution stirred overnight. Diethyl ether (100 mL) was added and the organic layer was separated, washed with water (2 × 100 mL), dried ($MgSO_4$), filtered and the solvent removed *in vacuo*. The resultant solid was dissolved in the minimum amount of chloroform and methanol (150 mL) was added to precipitate the desired imide. Purification was performed by flash chromatography (eluant: hexane/ethyl acetate).

Yield = 173 mg (15%); FTIR (KBr, $cm^{-1}$): 2954s, 2869m, 1776w, 1719m, 1465m, 1396m, 1366m, 1332m, 1230m, 1169m, 1109vs, 837m, 743m; $^1$H NMR (300 MHz, $CDCl_3$): $\delta$ 0.57–0.65 (m, 16H, $SiCH_2$/*i-Bu* $CH_2$), 0.92–0.96 (m, 42H, *i-Bu* $CH_3$), 1.78–1.87 (m, 9H, $CH_2$/*i-Bu* CH), 3.67 (t, $^3J_{H-H}$ = 7.20 Hz, 2H, $CH_2N$), 7.69–7.72 (m, 2H, CH), 7.84–7.86 (m, 2H, CH); $^{13}$C NMR (75.4 MHz, $CDCl_3$): $\delta$ 9.56 ($SiCH_2$), 22.14 ($CH_2$), 22.47, 23.85, 25.69 (*i-Bu*), 40.48 ($CH_2N$), 123.13 (CH), 132.20 (C–C), 133.80 (CH), 168.33 (C=O); $^{29}$Si NMR (59.6 MHz, $CDCl_3$): $\delta$ −68.02, −68.36, −68.56. HRMS calcd for $C_{39}H_{73}NNaO_{14}Si_8$1026.3083. Found 1026.3072. Elemental analysis calcd. (%) C 46.62, H 7.32, N 1.39. Found C 46.38, H 8.13, N 1.06. UV–Vis $\lambda_{max}$ ($\varepsilon$): 294 (2356).

### 2.3.2. Bis-phthalic POSS imide (**3a**)

Yield = 480 mg (37%); FTIR (KBr, $cm^{-1}$): 2954m, 2870m, 1774w, 1727m, 1465m, 1391m, 1366m, 1332w, 1230m, 1112vs, 838m, 743m; $^1$H NMR (300 MHz, $CDCl_3$): $\delta$ 0.57–0.60 (m, 32H, $SiCH_2$/*i-Bu* $CH_2$), 0.92–0.96 (m, 84H, *i-Bu* $CH_3$), 1.80–1.90 (m, 18H, $CH_2$/*i-Bu* CH), 3.72 (m, 4H, $CH_2N$), 8.27 (m, 2H, CH); $^{13}$C NMR (75.4 MHz, $CDCl_3$): $\delta$ 9.56 ($SiCH_2$), 22.04 ($CH_2$), 22.47, 23.82, 25.67 (*i-Bu*), 41.09 ($CH_2N$), 118.06, 137.23, 166.18 (C=O); $^{29}$Si NMR (59.6 MHz,$CDCl_3$): $\delta$ −68.01, −68.3, −68.51; HRMS calcd for $C_{72}H_{140}N_2NaO_{28}Si_{16}$ 1951.5799. Found 1951.5829. Elemental analysis calcd (%) C 45.02, H 7.45, N 1.39. Found C 44.78, H 7.31, N 1.45; UV–Vis $\lambda_{max}$ ($\varepsilon$ $M^{-1}$ $cm^{-1}$): 309 (2357).

### 2.3.3. Mono-naphthalic POSS imide (**2b**)

Yield = 107 mg (54%); FTIR (KBr, $cm^{-1}$): 2954m, 2906w, 2870w, 1703m, 1671m, 1591w, 1465w, 1437w, 1386w, 1365w, 1344w, 1316w, 1261w, 1244m, 1230w, 1200w, 1168w, 1109vs, 1032w, 837w, 802w, 782w, 743w; $^1$H NMR (300 MHz, $CDCl_3$): $\delta$ 0.57–0.61 (m, 14H, *i-Bu* $CH_2$), 0.70–0.76 (m, 2H, $SiCH_2$), 0.93–0.96 (m, 42H, *i-Bu* $CH_3$), 1.79–1.90 (m, 7H, *i-Bu* CH), 4.15 (t, $^3J_{H-H}$ = 6.6 Hz, 4H, $CH_2N$), 7.73 (t, $^3J_{H-H}$ = 7.8 Hz, 2H, CH), 8.18 (dd, $^3J_{H-H}$ = 8.40 Hz, $^2J_{H-H}$ = 0.9 Hz, 2H, CH), 8.58 (dd, $^3J_{H-H}$ = 7.80 Hz, $^2J_{H-H}$ = 0.9 Hz, 2H, CH); $^{13}$C NMR (75.4 MHz, $CDCl_3$): $\delta$ 9.72 ($SiCH_2$), 21.55 ($CH_2$), 22.39, 22.50, 23.84, 25.68, (*i-Bu*), 42.69 ($CH_2N$), 122.81, 126.85, 128.15, 131.04, 131.55, 133.68, 163.98 (C=O); $^{29}$Si NMR (59.6 MHz, $CDCl_3$): $\delta$ −68.05, −68.30, −68.40; HRMS calcd for $C_{43}H_{75}NNaO_{14}Si_8$ 1076.3239. Found 1076.3229 (theory); Elemental analysis calcd. (%) C 48.97, H 7.17, N 1.33; Found C 48.31, H 7.42, N 1.43; UV–Vis $\lambda_{max}$ ($\varepsilon$ $M^{-1}$ $cm^{-1}$): 335 (13846), 350 (15022); Fluorescence ($\lambda_{exc}$ = 335 nm, $CHCl_3$) 362, 380, 390 nm ($\Phi_F$ = 0.02).

### 2.3.4. Bis-naphthalic POSS imide (**3b**)

Yield = 368 mg (49%); FTIR (KBr, $cm^{-1}$): 2954m, 2870m, 1709m, 1672m, 1465w, 1366w, 1333m, 1230m, 1112vs, 838w, 743m; $^1$H NMR (300 MHz, $CDCl_3$): $\delta$ 0.57–0.61 (m, 28H, *i-Bu* $CH_2$), 0.69–0.75 (m, 4H, $SiCH_2$), 0.92–0.96 (m, 84H, *i-Bu* $CH_3$), 1.84 (n, $^3J_{H-H}$ = 6.3 Hz, 18H, $CH_2$/*i-Bu* CH), 3.67 (t, $^3J_{H-H}$ = 7.20 Hz, 4H, $NCH_2$), 8.76 (s, 4H, CH); $^{13}$C NMR (75.4 MHz, $CDCl_3$): $\delta$ 9.72 ($SiCH_2$), 21.55 ($CH_2$), 22.47, 23.85, 25.68 (*i-Bu*), 43.16 ($CH_2N$), 126.68, 130.86, 162.71 (C=O); $^{29}$Si NMR (59.6 MHz, $CDCl_3$): $\delta$ −68.03, −68.34, −68.54. HRMS calcd for $C_{76}H_{142}N_2NaO_{28}Si_{16}$ 2001.5955. Found 2001.5946 Elemental analysis calcd. (%) C 46.02, H 7.32, N 1.41; Found C 46.31, H 7.42, N 1.43; UV–Vis $\lambda_{max}$ ($\varepsilon$ $M^{-1}$ $cm^{-1}$): 342 (10084), 360 (15864), 381 (19153); Fluorescence ($\lambda_{exc}$ = 350 nm, $CHCl_3$) 350, 386, 404 nm ($\Phi_F$ = 0.05).

### 2.3.5. Bis-perylene POSS imide (**3c**)

Yield = 1.323 g (98%); FTIR (KBr, $cm^{-1}$): 2954m, 2869m, 1700m, 1663m, 1595m, 1465w, 1404w, 1342w, 1229m, 1110vs, 837w, 811w, 746m. $^1$H NMR (300 MHz, $CDCl_3$): $\delta$ 0.54–0.59 (m, 32H, $SiCH_2$/*i-Bu* $CH_2$), 0.93 (s, 84H, *i-Bu* $CH_3$), 1.83–1.90 (m, 18H, $CH_2$/*i-Bu* CH), 4.20 (m, 4H, $CH_2N$), 8.60 (br m, 8H, CH). $^{13}$C NMR (75.4 MHz, $CDCl_3$): $\delta$ 9.78 ($SiCH_2$), 21.57 ($CH_2$), 22.49, 23.93, 25.69, (*i-Bu*), 42.94 ($CH_2N$), 123.08, 123.30, 126.27, 129.23, 131.29, 134.38, 163.11 (C=O). $^{29}$Si (59.6 MHz, $CDCl_3$): $\delta$ −68.05, −68.14, −68.38; HRMS calcd for $C_{86}H_{146}N_2NaO_{28}Si_{16}$ 2127.628. Found 2127.6260; Elemental analysis calcd. (%) C 49.06, H 6.99, N 1.33; Found C 49.10, H 7.05, N 1.53; UV–Vis $\lambda_{max}$ ($\varepsilon$ $M^{-1}$ $cm^{-1}$) 459 (17157), 490 (48730), 526 nm

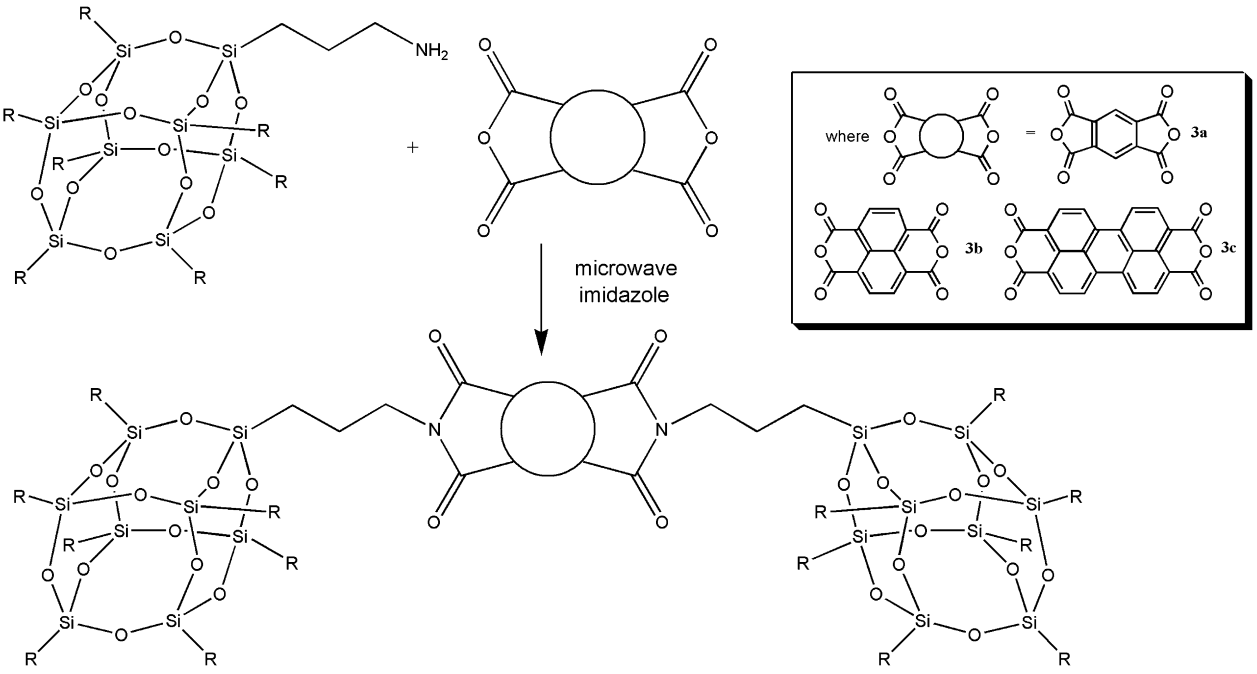


**Fig. 2.** Synthesis of bis-POSS diimides.

**Table 1**
FTIR of POSS imides.

| Compound | $\upsilon$(C=O)[34] ($cm^{-1}$) | $\upsilon$(C–N)[34] ($cm^{-1}$) |
|---|---|---|
| **1** | 1719 | 1465 |
| **2a** | 1727 | 1465 |
| **2b** | 1713 | 1415 |
| **3a** | 1703 | 1465 |
| **3b** | 1709, 1672 | 1465 |
| **3c** | 1700, 1663 | 1465 |

(80877); Fluorescence ($\lambda_{exc}$ = 450 nm, $CHCl_3$) 533, 575, 620 nm ($\Phi_F$ = 1.0).

## 3. Results and discussion

### 3.1. Synthesis

The condensation reactions of a variety of mono- and bis-anhydrides with a excess (4 equivalents) of mono-amino POSS was performed with the use of microwave radiation [31,32] in imidazole (Figs. 1 and 2) [33]. Thermal condensation of mono-amino POSS with a range of mono- and bis-anhydrides, including phthalic, perylene, naphthalene and biphenyl have recently been reported [35], however the use of microwave radiation the desired POSS imides to be synthesised in a greatly reduced timeframe.

The ability of aromatic cyclic anhydrides to undergo condensation reactions with primary amines to form the corresponding cyclic imides in good yields [38,39], implied that the most accessible route to aromatic POSS-functionalised imides, required a POSS cage peripherally substituted with a primary amine. The formation of mono-(3-aminopropyl) hepta-(*iso*-butyl) POSS adducts (hereafter referred to as mono-amino POSS) has previously been achieved through the condensation of 3-aminopropyltriethoxysilane with the incompletely condensed POSS species, *i*-$Bu_7Si_7O_9(OH)_3$, in the presence of tetrabutylammonium hydroxide, to yield *i*-$Bu_7Si_7O_{12}(CH_2CH_2CH_2NH_2)$ (**1** in Fig. 1) [30].

FTIR spectra of the resulting POSS imides exhibited a band at approximately 1465 $cm^{-1}$ for the mono- and bis-POSS derivatives, assigned to the stretching mode of the C–N bond in the imide functionality [40,41]. The POSS imides exhibited a carbonyl stretching band from 1700 to 1727 $cm^{-1}$, with the second carbonyl stretching band only present in the naphthalic and perylene diimides at 1672 and 1663 $cm^{-1}$, respectively [42]. The FTIR bands of interest of the POSS imides are detailed in Table 1.

The $^1$H NMR spectra displayed little change in the resonances of the isobutyl chains of the POSS cage with resonances generally apparent as multiplets at approximately ~$\delta$ 0.6 (16H, $SiCH_2$/*i-Bu* $CH_2$), 0.95 (42H, *i-Bu* $CH_3$) and 1.85 (9H, $CH_2$/*i-Bu* CH). Resonances of the propyl chain were generally obscured, with the exception of the $CH_2N$ resonance, which was apparent at approximately $\delta$ 3.65–4.20 ppm. This resonance exhibited a downfield shift of 1 ppm for the phthalic monoimide and phthalic, naphthalic and biphenyl diimides and 1.4 ppm for the naphthalic monoimide and perylene diimide. Comparable resonance shifts in similar compounds have been reported in the literature [40,43–45]. The aromatic resonances were evident in the range $\delta$ 7.50–8.60 ppm, as expected.

**Table 2**
$^{29}$Si NMR of POSS imides.

| Compound | $^{29}$Si NMR |
|---|---|
| **1** | −67.64, −68.06, −68.26 |
| **2a** | −68.02, −68.36, −68.56 |
| **2b** | −68.01, −68.30, −68.51 |
| **3a** | −68.05, −68.30, −68.40 |
| **3b** | −68.03, −68.34, −68.54 |
| **3c** | −68.05, −68.14, −68.38 |

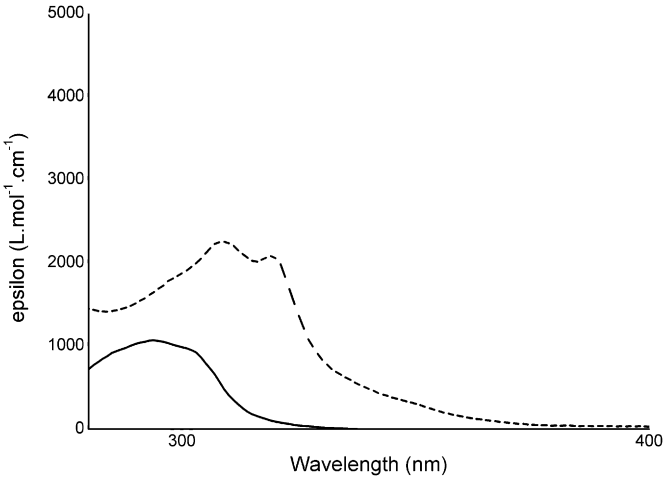


**Fig. 3.** UV–Vis of phthalic mono- and diimide [(—) absorption (- - -) emission] in chloroform.

$^{13}$C NMR exhibited resonances of the isobutyl carbons at ~$\delta$ 24.00, 25.80 and 27.20 ppm, with resonances of the propyl carbons apparent at $\delta$ 9.40–9.80 ($SiCH_2$), 21.50–22.70 ($CH_2$) and 40.70–44.90 ppm ($CH_2N$). Downfield shifts were observed in the $SiCH_2$ resonance (0.20 ppm), and upfield shifts of the $CH_2$ (0.41 ppm) and $CH_2N$ (3.42 ppm) resonances. Comparable shifting patterns were apparent in the bis-propyl triethoxysilane phthalic derivative (0.1, 5.4 and 4.2 ppm), relative to (3-aminopropyl)triethoxysilane [44]. The electron-withdrawing properties of a POSS cage are comparable to those associated with a trifluoromethyl ($CF_3$) group [46,47], therefore, the adjacent propyl chain carbons experienced increased deshielding, with reduced upfield shifts of the propyl chain resonances of phthalic POSS imides observed [48]. Aromatic ($\delta$ 118.00–145.10 ppm) and carbonyl (162.70–168.40 ppm) resonances were observed in the expected regions.

The $^{29}$Si NMR resonances of the POSS amines and imides are detailed in Table 2. All POSS imides exhibited resonances characteristic of the functionalised POSS cages, with upfield shifts of approximately 0.3 ppm present in resonances of all mono- and bis-imides following reaction of the amino group.

The compounds were further characterized by High Resolution Mass Spectrometry and elemental analysis, with the close

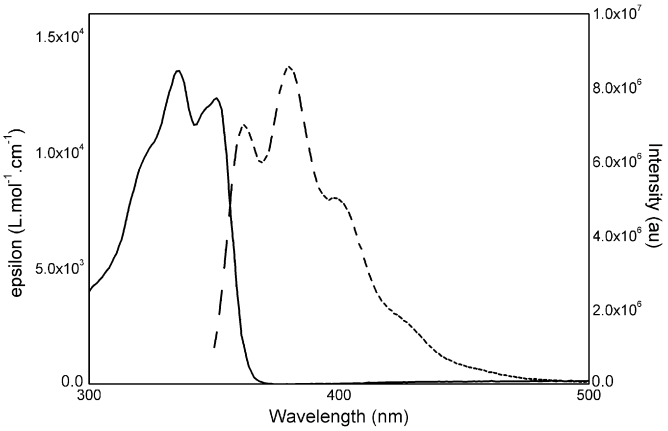


**Fig. 4.** UV–Vis/fluoro spectra of naphthalic monoimide [(—) absorption (- - -) emission] in chloroform.

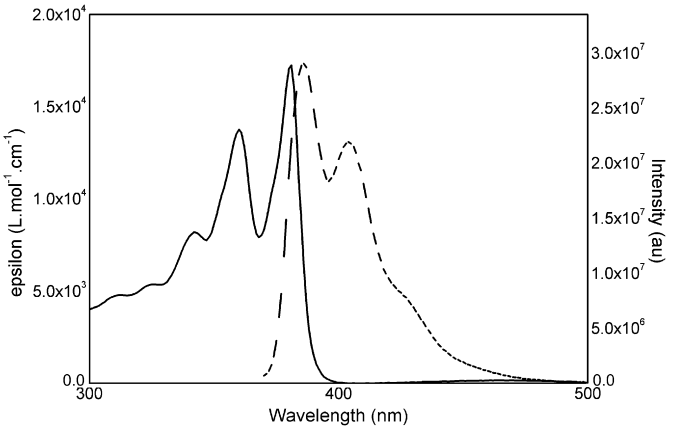


**Fig. 5.** UV–Vis/fluoro spectra of naphthalic diimide [(—) absorption (- - -) emission] in chloroform.

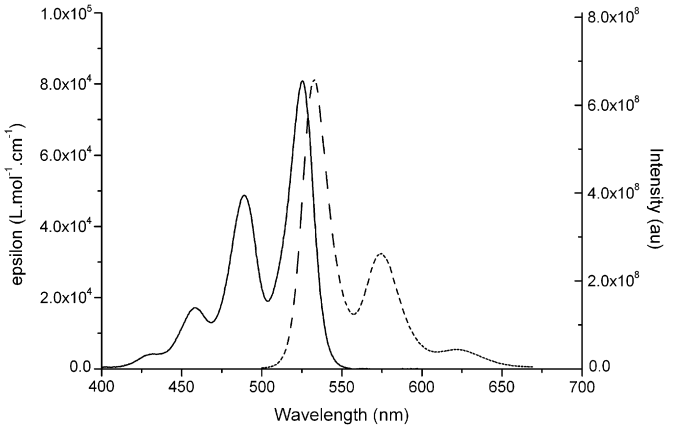


**Fig. 6.** UV–Vis and fluorescence spectra of perylene diimide [(—) absorption (- - -) emission] in chloroform.

correlation between the experimental and theoretical results providing further confirmation of the formation of the desired POSS imides (for full details see Experimental).

### 3.2. Spectroscopic properties

The $\pi-\pi^*$ absorption maxima of phthalyl monoimide **2a** and diimide **3a** (Fig. 3) were apparent at 294 nm (2356) and 309 nm (2357), with the maxima position and extinction coefficients being comparable to other mono- (300 nm, 1840) [49] and diimide (308 nm, 4800; 310 nm, 4000; 320 nm, 2400) examples in the literature [50,51]. Higher transitions were not observed due to the insolubility of the compound in the required solvents [49].

**Table 3**
UV and fluorescence data of POSS diimides.

| Compound | $\lambda_{max}$ (nm) | Extinction Coefficient (L mol$^{-1}$ cm$^{-1}$) | $\lambda_{em}$ (nm) | Quantum Yield |
|---|---|---|---|---|
| **2a** | 294 | 2356 | – | – |
| **2b** | 309 | 2357 | – | – |
| **3a** | 335, 350 | 13846, 15022 | 362, 380, 390 | 0.02 |
| **3b** | 342, 360, 381 | 10084, 15864 | 350, 386, 404 | 0.05 |
| **3c** | 459, 490, 526 | 17157, 48730, 80877 | 533, 575, 620 | 1.0 |

The UV–Vis and fluorescence spectra of naphthalyl monoimide **2b** are depicted in Fig. 4. The absorption spectra of **2b** exhibited maxima at 335 and 350 nm. Literature examples of alkyl mono-naphtha imides exhibited absorption maxima at approximately 330 nm and 345 nm; with the exact position of the maxima being solvent dependent [52,53]. Excitation of **2b** yielded emission bands with a maximum at 380 nm and shoulder bands at 362 and 398 nm. The fluorescence observed was extremely weak compared to that of perylenes, with a quantum yield ($\Phi_F$) of 0.02 observed. The weak fluorescence of **2b** was similar to that of other mono-naphthalene imides in the literature, which typically possess quantum yields of approximately 0.01 [52], with two overlapping electronic levels of the naphthalene structure postulated as being responsible for the fluorescence deactivation [54].

The UV–Vis and fluorescence spectra of naphthalyl diimide **3b** are depicted in Fig. 5. The absorption spectrum of **3b** exhibited maxima at 342, 360 and 381 nm, analogous to literature di-naphthalene derivatives (342, 360 and 380 nm) [55–57]. Excitation of **3b** yielded emission bands with maxima at 386 and 404 nm. The resultant weak fluorescence ($\Phi_F = 0.05$) was comparable to that present in other naphthalic diimides, which typically possess quantum yields of 0.035 [55,58–60].

The UV–Vis and fluorescence spectra of the POSS substituted perylene diimide **3c** are depicted in Fig. 7. The UV–Vis spectrum of **3c** displayed three characteristic absorption bands at 459, 490 and 526 nm [41,42,61]. The band at 526 nm represented a lowest energy transition from the ground state (zero vibrational level) to the first excited state, whilst the subsequent maxima at 490 and 459 nm corresponded to transitions to the various excited vibrational levels of the first electronic excited state, consistent with previous findings [62,63]. Aggregation of perylene diimides is characterized through the appearance of a broad band in the absorption spectrum at ~580 nm, observed at even $10^{-5}$ M concentrations, in a range of solvents [58,64]. The particular spectrum shown in Fig. 6 was obtained with a concentration of $1.8 \times 10^{-6}$ M, in order to obtain the fluorescence spectrum, however higher concentrations were also measured, with no change in the absorption profile evident. Spectra were also obtained in chloroform, with no change in band position or structure evident, as little solvatochromism is exhibited

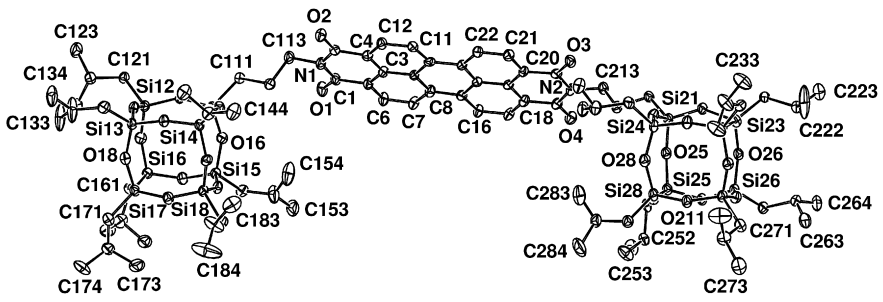


**Fig. 7.** Plot of the molecule of **3c**. Hydrogen atoms have been removed for clarity.

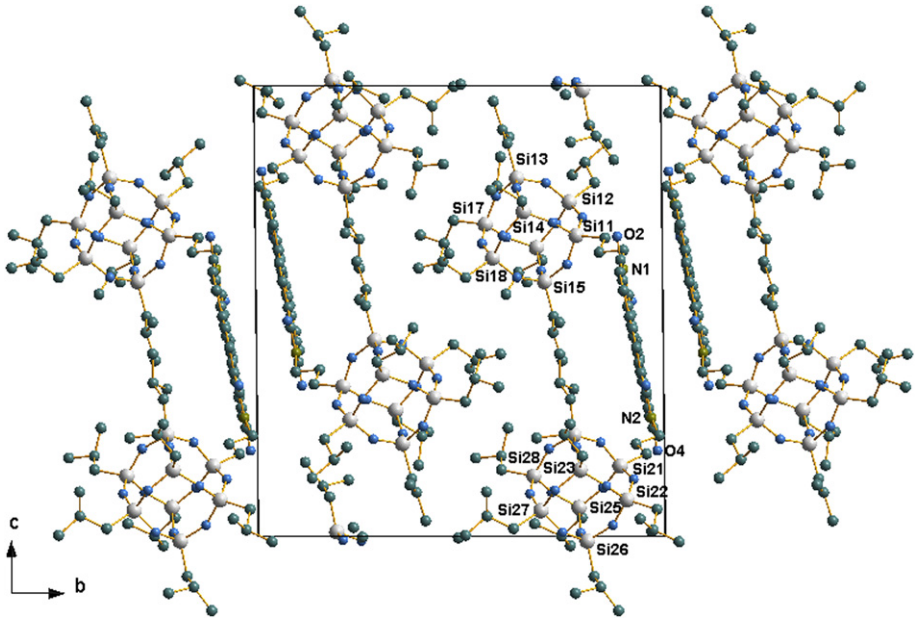


**Fig. 8.** Unit cell contents of **3c** projected along the *a* axis.

in perylene diimides [65]. The absence of a band at 580 nm implies there is no aggregation present in solution at these concentrations.

Excitation of **3c** resulted in an emission maximum at 533 nm, with the first and second red-shifted vibrational bands at 575 and 620 nm ($\Phi_F = 1.0$) (Fig. 7). This quantum yield was comparable to values reported for a range of perylene derivatives in the literature, which are generally upwards of 0.9, and typically closer to unity [3,41,64,66–71]. Aggregation also causes a dramatic reduction of the fluorescence quantum yield, with aggregating diimides such as *p*-hydroxyphenyl and *p*-cyanophenyl perylene diimides possessing quantum yields of 0.2 and 0.136, respectively [58,64]. In contrast, 'non-aggregating' perylene diimides exhibit quantum yields in the region 0.8–1 [3,41,64,66–71].

The UV and fluorescence properties of the functionalised POSS imides are summarized in Table 3. The optical properties were consistent with those exhibited by related compounds in the literature.

### 3.3. Single crystal X-ray structure determination

Single crystals suitable for X-ray crystallography were grown from the vapour diffusion of methanol into a chloroform solution of **3c**. X-ray crystallographic data was collected at 100(2) K using CuKα radiation ($\lambda = 1.5418$ Å). Following multi-scan absorption corrections and solution by direct methods, the structure was refined against $F^2$ by full-matrix least-squares using the program SHELXL-97[21]. All hydrogen atoms were added at calculated positions and refined by use of riding models with the isotropic displacement parameters based on those values of the parent atoms. Anisotropic displacement parameters were employed for all non-hydrogen atoms. The molecular structure of **3c** is depicted in Fig. 8 where ellipsoids have been drawn at the 20% probability level. A summary

**Table 4**
Crystal data and refinement details for **3c**.

| | |
|---|---|
| Molecular formula | $C_{86}H_{146}N_2O_{28}Si_{16}$ |
| Formula weight | 2105.44 |
| Crystal description | Plate |
| Crystal colour | Red |
| Crystal dimensions (mm) | 0.33 × 0.07 × 0.011 |
| Crystal system | Triclinic |
| Space group | $P\bar{1}$ |
| a [Å] | 11.464(3) |
| b [Å] | 20.859(7) |
| c [Å] | 23.103(2) |
| α [°] | 89.46(2) |
| β [°] | 81.78(2) |
| γ [°] | 81.96(2) |
| V [Å$^3$] | 5414(2) |
| Z | 2 |
| $D_{calc}$[g/cm$^3$] | 1.292 |
| Temperature (K) | 100(2) |
| Range in $\theta$ [°] | 2.87–65.70 |
| Reflections collected | 61,627 |
| Independent reflections | 18,388 |
| Reflections ($I > 2\sigma(I)$) | 6576 |
| Parameters refined | 1217 |
| *R*1 ($I > 2\sigma(I)$) | 0.0669 |
| *wR*2 (all data) | 0.1954 |
| Goodness-of-fit on $F^2$ | 0.849 |

**Table 5**
Bond distances of **3c** and literature perylene diimides [65].

| Bond | POSS distance (Å) | Bond | POSS distance (Å) | Literature avg. distance (Å)[73] |
|---|---|---|---|---|
| C1–N1 | 1.364(8) | C23-N2 | 1.398(8) | 1.38 |
| C1–C2 | 1.495(8) | C18-C23 | 1.489(9) | 1.47 |
| C2–C3 | 1.417(9) | C18–C19 | 1.396(8) | 1.41 |
| C2–C6 | 1.355(9) | C17–C18 | 1.377(9) | 1.36 |
| C3–C4 | 1.382(8) | C19–C20 | 1.411(8) | 1.43 |
| C3–C9 | 1.413(8) | C14–C19 | 1.427(8) | 1.41 |
| C4–C5 | 1.499(8) | C20–C24 | 1.493(8) | 1.47 |
| C4–C12 | 1.377(9) | C20–C21 | 1.345(8) | 1.37 |
| C5–N1 | 1.405(8) | C24–N2 | 1.357(8) | 1.41 |
| C6–C7 | 1.384(8) | C16–C17 | 1.408(8) | 1.39 |
| C7–C8 | 1.386(9) | C13–C16 | 1.370(8) | 1.40 |
| C8–C9 | 1.434(9) | C13–C14 | 1.430(8) | 1.42 |
| C8–C13 | 1.446(8) | C10–C15 | 1.474(8) | 1.46 |
| C9–C10 | 1.441(8) | C14–C15 | 1.418(8) | 1.43 |
| C10–C11 | 1.380(8) | C15–C22 | 1.383(8) | 1.37 |
| C11–C12 | 1.412(8) | C21–C22 | 1.401(8) | 1.40 |
| C113–N1 | 1.478(7) | C213–N2 | 1.478(7) | 1.51 |
| C111–C112 | 1.543(8) | C211–C212 | 1.549(7) | – |
| C112–C113 | 1.502(8) | C212–C213 | 1.521(8) | – |
| C113–N1 | 1.478(7) | C213–N2 | 1.478(7) | – |

**Table 6**
Bond angles of the perylene groups for **3c**.

| Atoms | Angle (°) |
|---|---|
| Si11–C111–C112 | 113.5(5) |
| C111–C112–C113 | 108.7(5) |
| N1–C113–C112 | 113.2(5) |
| C1–N1–C5 | 123.9(6) |
| N1–C1–C2 | 118.7(6) |
| C1–C2–C3 | 119.7(6) |
| C2–C3–C4 | 119.5(6) |
| C3–C4–C5 | 121.9(6) |
| C4–C5–N1 | 116.3(6) |
| C–C–C perylene | 120.02 |
| Si21–C211–C212 | 113.7(4) |
| C211–C212–C213 | 109.8(5) |
| N2–C213–C212 | 113.2(5) |
| C23–N2–C24 | 125.1(6) |
| N2–C23–C18 | 115.5(6) |
| C23–C18–C19 | 121.6(6) |
| C18–C19–C20 | 120.2(6) |
| C19–C20–C24 | 118.6(6) |
| C20–C24–N2 | 118.8(6) |

of crystallographic data is given in Table 4, with interatomic parameters detailed in Tables 5 and 6. Full details of the structure determinations (except structure factors) have been deposited with the Cambridge Crystallographic Data Centre as CCDC 814303.

Molecules of **3c** crystallised in the triclinic space group $P\bar{1}$. The nitrogen bound POSS cages essentially adopted a *cis*-like conformation. This allowed for optimum packing of the molecule within the unit cell (Fig. 9), as a POSS cage of an adjacent molecule was able to slot within the cavity between two POSS cages of one molecule of **3c**, thus allowing for the $\pi-\pi$ stacking of adjacent perylene cores on the neighbouring surface of the molecule.

X-ray studies of several single crystal perylene structures have shown that parent perylene diimides exhibit flat $\pi$-systems [65,72–75]. The numbering scheme used to describe the POSS perylene diimide core used in the structural description of **3c** is shown in Fig. 9.

The average bond distances observed in a range of perylene diimide crystal structures together with the bond distances observed in the POSS perylene diimide synthesised in the present work are detailed in Table 5 [65]. It was evident from the bond distances of the perylene POSS that the two naphthalene half units exhibited similar bond distances with no significant differences between the literature values and those observed in the perylene POSS structure. Thus the perylene core of the molecule was consistent with other perylene crystal structures described in the literature. The bond angles associated with the perylene moiety are detailed in Table 6, with angles falling within the ranges reported in the literature [74,76,77].

The bond angles associated with the propyl chains of the POSS cages were also in agreement with those reported in the literature [78–81]. The lack of substitution in the bay region of the perylene

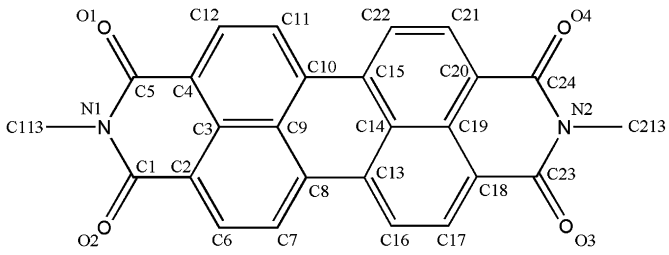


**Fig. 9.** Numbering scheme used for perylene **POSS** imide **3c**.

POSS diimide implied that the aromatic perylene core, similar to other previously investigated perylene diimides, exhibited an almost planar, although slightly bowed, geometry. The dihedral angles between the peripheral $C_5N$ rings and the central $C_6$ ring are 2.9(2) and 2.0(2)°.

The steric requirement of the imide substituent dictates the stacking distance and longitudinal and transverse offset of the perylene diimides [72–75]. The unit cell, (Fig. 9), shows the bulky POSS groups being present in a *cis*-like coordination, but also indicates that the central perylene core is interacting with an adjacent perylene moiety through $\pi-\pi$ interactions. The parallel separation distance between neighbouring perylene moieties of **3c** (3.39 Å), was comparable to other perylene diimides in the literature (3.34–3.55 Å) [65,72–75]. The incorporation of $\pi$-electron perylenes onto the periphery of the POSS cage effectively isolated the chromophores from each other by both steric and electronic effects, due to the rigid and bulky core and the non-conjugated nature of the siloxane bond [24].

## 4. Conclusion

A range of POSS imides have been synthesised through the condensation of POSS amines with a variety of mono- and bis-anhydrides. The POSS imides were characterized by $^{1}H$, $^{13}C$ and $^{29}Si$ NMR, ESI mass spectrometry, FTIR, elemental analysis, UV–VIS and fluorescence spectrophotometry and. The POSS perylene diimide was further characterized by single crystal X-ray crystallography. The various methods of characterization confirmed the formation of the desired POSS imides. The X-ray crystal structure of the perylene diimide confirmed that the incorporation of perylene functionality onto the periphery of the bulky POSS molecule partially isolated the perylene moieties and thus reduced the aggregation of the aromatic perylene cores in the solid state.

## Acknowledgements

This work was largely funded by the Australian Research Council Discovery Scheme (DP0449692).

## References

[1] Zhan X, Facchetti A, Barlow S, Marks TJ, Ratner MA, Wasielewski MR, et al. Rylene and related diimides for organic electronics. Adv Mater 2011;23(2):268–84.
[2] Ego C, Marsitzky D, Becker S, Zhang J, Grimsdale AC, Mullen K, et al. Attaching perylene dyes to polyfluorene: three simple, efficient methods for facile color tuning of light-emitting polymers. J Am Chem Soc 2002;125(2):437–43.
[3] Sadrai M, Hadel L, Sauers RR, Husain S, Krogh-Jespersen K, Westbrook JD, et al. Lasing action in a family of perylene derivatives: singlet absorption and emission spectra, triplet absorption and oxygen quenching constants, and molecular mechanics and semiempirical molecular orbital calculations. J Phys Chem 1992;96(20):7988–96.
[4] O'Neil MP, Niemczyk MP, Svec WA, Gosztola D, Gaines GL, Wasielewski MR. Picosecond optical switching based on biphotonic excitation of an electron donor–acceptor–donor molecule. Science 1992;257(5066):63–5.
[5] Law KY. Organic photoconductive materials: recent trends and developments. Chem Rev 1993;93(1):449–86.
[6] Schenning APHJ, van Herrikhuyzen J, Jonkheijm P, Chen Z, Wurthner F, Meijer EW. Photoinduced electron transfer in hydrogen-bonded oligo(p-phenylene vinylene) perylene bisimide chiral assemblies. J Am Chem Soc 2002;124(35):10252–3.
[7] Langhals H, Esterbauer AJ, Walter A, Riedle E, Pugliesi I. Förster resonant energy transfer in orthogonally arranged chromophores. J Am Chem Soc 2010;132(47):16777–82.
[8] Mathew S, Johnston MR. The synthesis and characterisation of a free-base porphyrin–perylene dyad that exhibits electronic coupling in both the ground and excited states. Chem Eur J 2009;15(1):248–53.
[9] Struijk CW, Sieval AB, Dakhorst JEJ, van Dijk M, Kimkes P, Koehorst RBM, et al. Liquid crystalline perylene diimides: architecture and charge carrier mobilities. J Am Chem Soc 2000;122(45):11057–66.
[10] Dimitrakopoulos CD, Malenfant PRL. Organic thin film transistors for large area electronics. Adv Mater 2002;14(2):99–117.

[11] Lee SK, Zu Y, Herrmann A, Geerts Y, Mullen K, Bard AJ. Electrochemistry, spectroscopy and electrogenerated chemiluminescence of perylene, terrylene, and quaterrylene diimides in aprotic solution. J Am Chem Soc 1999;121(14): 3513–20.
[12] Würthner F. Plastic transistors reach maturity for mass applications in microelectronics. Angew Chem Int Ed 2001;40(6):1037–9.
[13] Zhang X, Rehm S, Safont-Sempere MM, Würthner F. Vesicular perylene dye nanocapsules as supramolecular fluorescent pH sensor systems. Nat Chem 2009;1(8):623–9.
[14] Yakimov A, Forrest SR. High photovoltage multiple-heterojunction organic solar cells incorporating interfacial metallic nanoclusters. Appl Phys Lett 2002;80:1667.
[15] Mathew S, Imahori H. Tunable, strongly-donating perylene photosensitizers for dye-sensitized solar cells. J Mater Chem 2011;21(20):7166–74.
[16] Würthner F, Thalacker C, Diele S, Tschierske C. Fluorescent J-type aggregates and thermotropic columnar mesophases of perylene bisimide dyes. Chem Eur J 2001;7:2245.
[17] Würthner F, Thalacker C, Sautter A, Schartl W, Ibach W, Hollricher O. Hierarchical self-organization of perylene bisimide–melamine assemblies to fluorescent mesoscopic superstructures. Chem Eur J 2000;6:3871.
[18] Zheng Q, Huang J, Sarjeant A, Katz HE. Pyromellitic diimides: minimal cores for high Mobility n-Channel transistor semiconductors. J Am Chem Soc 2008; 130(44):14410–1.
[19] Zhang C, Laine RM. Hydrosilylation of allyl alcohol with $[HSiMe_2OSiO_{1.5}]_8$: octa(3-hydroxypropyldimethylsiloxy)octasilsesquioxane and Its octamethacrylate derivative as potential precursors to hybrid nanocomposites. J Am Chem Soc 2000;122:6979–88.
[20] Tamaki R, Tanaka Y, Asuncion MZ, Choi J, Laine RM. Octa(aminophenyl)silsesquioxane as a nanoconstruction site. J Am Chem Soc 2001;123:12416–7.
[21] Zhang C, Babonneau F, Bonhomme C, Laine RM, Soles CL, Hristov A, et al. Highly porous polyhedral silsesquioxane polymers. Synthesis and characterization. J Am Chem Soc 1998;120:8380.
[22] Costa ROR, Vasconcelos WL, Tamaki R, Laine RM. Organic/inorganic nanocomposite star polymers via atom transfer radical polymerization of methyl methacrylate using octafunctional silsesquioxane cores. Macromolecules; 2001:5398.
[23] Cho HJ, Hwang DH, Lee JI, Jung YK, Park JH, Lee J, et al. Electroluminescent polyhedral oligomeric silsesquioxane-based nanoparticle. Chem Mater 2006; 18(16):3780–7.
[24] Imae I, Kawakami YJ. Unique photoluminescence property of a novel perfectly carbazole-substituted POSS. J Mater Chem 2005;15:4581–3.
[25] Xiao Y, Liu L, He C, Chin WS, Lin T, Mya KY, et al. Nano-hybrid luminescent dot: synthesis, characterization and optical properties. J Mater Chem 2006;16: 829–36.
[26] Lee J, Cho HJ, Cho NS, Hwang DH, Kang JM, Lim E, et al. Enhanced efficiency of polyfluorene derivatives: organic-inorganic hybrid polymer light-emitting diodes. J Polym Sci A Polym Chem 2006;44(9):2943–54.
[27] Takagi K, Kunii S, Yuki Y. Synthesis and photophysical properties of polyfluorenes bearing silicon-based functional groups. J Polym Sci A Polym Chem 2005;43(10):2119–27.
[28] Lin WJ, Chen WC, Wu WC, Niu YH, Jen AKY. Synthesis and optoelectronic properties of starlike polyfluorenes with a silsesquioxane core. Macromolecules 2004;37:2335–41.
[29] Armarego WLF, Chai CLL. Purification of laboratory chemicals. 5th ed. Butterworth-Heinemann; 2003.
[30] Carsten J, Adolf K. Method for producing functionalised oligomeric silsesquioxanes and the use of the same; 2003. WO03042223.
[31] Kacprzak K. Rapid and convenient microwave-assisted synthesis of aromatic imides and N-hydroxymethylimides. Synth Commun 2003;33(9):1499–507.
[32] Liu MO, Tai CH, Chen CW, Chang WC, Hu AT. The fluorescent and photoelectric conversion properties of porphyrin-perylene tetracarboxylic complex. J Photochem Photobiol A Chem 2004;163(1–2):259–66.
[33] Bowden NB, Willets KA, Moerner WE, Waymouth RM. Synthesis of fluorescently labeled polymers and their use in single-molecule imaging. Macromolecules 2002;35(21):8122–5.
[34] Klán P, Hájek M, Církva V. The electrodeless discharge lamp: a prospective tool for photochemistry: part 3. The microwave photochemistry reactor. J Photochem Photobiol A Chem 2001;140(3):185–9.
[35] Jegenathan SG, Suruliappa G, Bramer D, Kote R, Maladkar GJ. In: Corporation CSC, editor. Novel polyhedral oligomeric silsesquioxane (POSS) based fluorescent colourants; 2008. US 2008/0029739.
[36] Tamaki R, Choi J, Laine RM. A polyimide nanocomposite from octa(aminophenyl)silsesquioxane. Chem Mater 2003;15:793–7.
[37] Leu CM, Mahesh Reddy G, Wei KH, Shu CF. Synthesis and dielectric properties of polyimide-chain-end tethered polyhedral oligomeric silsesquioxane nanocomposites. Chem Mater 2003;15:2261–5.
[38] Nagao Y, Misono T. Synthesis and reactions of perylenecarboxylic acid derivatives. VIII. Synthesis of N-alkyl-3,4:9,10-perylenetetracarboxylic monoanhydride monoimide. Bull Chem Soc Jpn 1981;54(4):1191–4.
[39] Langhals H. Control of the interactions in multichromophores: novel concepts. Perylene bis-imides as components for larger functional units. Helv Chim Acta 2005;88(6):1309–43.
[40] Luo Y, Lin J, Duan H, Zhang J, Lin C. Self-directed assembly of photoactive perylenediimide-bridged silsesquioxane into a superlong tubular structure. Chem Mater 2005;17(9):2234–6.
[41] Icil H, Arslan E. Synthesis and spectroscopic properties of highly pure perylene fluorescent dyes. Spec Lett 2001;34(3):355–63.
[42] Feiler L, Langhals H, Polborn K. Synthesis of perylene-3,4-dicarboximides – novel highly photostable fluorescent dyes. Lieb Annal 1995;7:1225–44.
[43] Wright ME, Petteys BJ, Guenthner AJ, Yandek GR, Baldwin LC, Jones C, et al. Synthesis and chemistry of a monotethered-poss bis(cyanate) ester: thermal curing of micellar aggregates leads to discrete nanoparticles. Macromolecules 2007;40(11):3891–4.
[44] Bes L, Rousseau A, Boutevin B, Mercier R, Sillion B. Syntheses and characterizations of bis(trialkoxysilyl)oligoimides, 1 synthesis of model compounds and study of the thermal self-crosslinking. Macromol Chem Phys 2001;202(6): 933–42.
[45] Rampazzo E, Brasola E, Marcuz S, Mancin F, Tecilla P, Tonellato U. Surface modification of silica nanoparticles: a new strategy for the realization of self-organized fluorescence chemosensors. J Mater Chem 2005;15(27–28): 2687–96.
[46] Feher FJ, Budzichowski TA, Blanski RL, Weller KJ, Ziller JW. Facile syntheses of new incompletely condensed polyhedral oligomeric oligosilsesquioxanes: [(c-C5H9)7Si7O9(OH)3], [(c-C7H13)7Si7O9(OH)3] and [(c-C5H9)6Si6O7(OH)4]. Organomet 1991;10:2526–8.
[47] Feher FJ, Budzichowski TA. New polyhedral oligosilsesquioxanes via the catalytic hydrogenation of aryl-containing silsesquioxanes. J Organomet Chem 1989;373:153–63.
[48] Thieuleux C, Quadrelli EA, Basset JM, Döbler J, Sauer J. Methane activation by silica-supported Zr(IV) hydrides: the dihydride [(SiO)2ZrH2] is much faster than the monohydride [(SiO)3ZrH]. Chem Commun 2004;15:1729–31.
[49] Gawronski J, Kazmierczak F, Gawronska K, Rychlewska U, Norden B, Holmen A. Excited states of the phthalimide chromophore and their exciton couplings: a tool for stereochemical assignments. J Am Chem Soc 1998; 120(46):12083–91.
[50] Ishida H, Wellinghoff ST, Baer E, Koenig JL. Spectroscopic studies of poly[N, N'-bis(phenoxyphenyl)pyromellitimide]. 1. Structures of the polyimide and three model compounds. Macromolecules 1980;13:826–34.
[51] Hasegawa M, Shindo Y, Sugimura T, Ohshima S, Horie K, Kochi M, et al. Photophysical processes in aromatic polyimides. Studies with model compounds. J Polym Sci Part B Polym Phys 1993;31(11):1617–25.
[52] Prezhdo OV, Uspenskii BV, Prezhdo VV, Boszcyzk W, Distanov VB. Synthesis and spectral-luminescent characteristics of N-substituted 1,8-naphthalimides. Dyes Pigm 2007;72:42–6.
[53] Adachi M, Murata Y, Nakamura S. Spectral similarity and difference of naphthalenetetracarboxylic dianhydride, perylenetetracarboxylic dianhydride, and their derivatives. J Phys Chem 1995;99(39):14240–6.
[54] Kim KM, Adachi KA, Chujo Y. Polymer hybrids of functionalized silsesquioxanes and organic polymers utilising the sol-gel reaction of tetramethoxysilane. Polymer 2003;43:1171–5.
[55] Langhals H, Jaschke H. Naphthalene amidine imide dyes by transamination of naphthalene bisimides. Chem Eur J 2006;12(10):2815–24.
[56] Lee YL, Hsu HL, Chen SY, Yew TR. Solution-processed naphthalene diimide derivatives as n-type semiconductor materials. J Phys Chem C 2008;112(5): 1694–9.
[57] Erten S, Posokhov Y, Alp S, Icli S. The study of the solubility of naphthalene diimides with various bulky flanking substituents in different solvents by UV–vis spectroscopy. Dyes Pigm 2005;64:171–8.
[58] Uzun D, Ozser E, Yuney K, Icil H, Demuth M. Synthesis and photophysical properties of N, N′-bis(4-cyanophenyl)-3,4,9,10-perylenebis(dicarboximide) and N, N′-bis(4-cyanophenyl)-1,4,5,8-naphthalenediimide. J Photochem Photobiol A Chem 2003;156:45–54.
[59] Barros TC, Brochsztain S, Toscano VG, Filho PB, Politi MJ. Photophysical characterization of a 1,4,5,8-naphthalenediimide derivative. J Photochem Photobiol A Chem 1997;111(1–3):97–104.
[60] Posokhov Y, Alp S, Köz B, Dilgin Y, Icli S. Photophysical properties and electrochemistry of the N, N'-bis-n-butyl derivative of naphthalene diimide. Turk J Chem 2004;28:415–24.
[61] Balakrishnan K, Datar A, Oitker R, Chen H, Zuo J, Zang L. Nanobelt self-assembly from an organic n-type semiconductor: propoxyethyl-PTCDI. J Am Chem Soc 2005;127(30):10496–7.
[62] Sapagovas VJ, Gaidelis V, Kovalevskij V, Undzenas A. 3,4,9,10-Perylenetetracarboxylic acid derivatives and their photophysical properties. Dyes Pigm 2006;71:178–87.
[63] Langhals H, Demmig S, Huber H. Rotational barriers in perylene fluorescent dyes. Spectrochim Acta 1988;44A:1189.
[64] Pasaogullari N, Icil H, Demuth M. Symmetrical and unsymmetrical perylene diimides: their synthesis, photophysical and electrochemical properties. Dyes Pigm 2006;69(3):118–27.
[65] Wurthner F. Perylene bisimide dyes as versatile building blocks for functional supramolecular architectures. Chem Commun; 2004:1564–79.
[66] Karapire C, Timur C, Icli S. A comparative study of the photophysical properties of perylenediimides in liquid phase, PVC and sol-gel host matrices. Dyes Pigm 2003;56:135–43.
[67] Langhals H, Karolin J, Johansson L. Spectroscopic properties of new and convenient standards for measuring fluorescence quantum yields. J Chem Soc Faraday Trans 1998;94:2919–22.
[68] Sadrai M, Bird GR. A new laser dye with potential for high stability and a broad band of lasing action: perylene-3,4,9,10-tetracarboxylic acid-bis-N, N′(2′,6′ xylidyl)diimide. Opt Commun 1984;51:62–4.

[69] Lohmannsroben HG, Langhals H. Laser performance of perylene bis(dicarboximide) dyes with long secondary alkyl chains. Appl Phys B 1989;48:449–52.
[70] Reisfeld R, Seybold G. Solid-State tunable lasers in the visible, based on luminescent photoresistant heterocyclic colorants. Chimia 1990;44:295.
[71] Ford WE, Kamat PV. Photochemistry of 3,4,9,10-perylenetetracarboxylic dianhydride dyes. 3. Singlet and triplet excited-state properties of the bis(2,5-ditert-butylphenyl)imide derivative. J Phys Chem 1987;91:6373–80.
[72] Graser F, Hadicke E. Kristallstruktur und Farbe bei Perylen-3,4:9,10-bis(dicarboximid)-Pigmenten. Lieb Annal Chem; 1980:1994–2011.
[73] Graser F, Hadicke E. Kristallstruktur und Farbe bei Perylen-3,4:9,10-bis(dicarboximid)-Pigmenten. Lieb Annal Chem; 1984:483–94.
[74] Hadicke E, Graser F. Structures of eleven perylene-3,4:9,10-bis(dicarboximide) pigments. Acta Crystallogr C 1986;42:195–8.
[75] Klebe G, Graser F, Hadicke E, Berndt J. Crystallochromy as a solid-state effect: correlation of molecular conformation, crystal packing and colour in perylene-3,4:9,10-bis(dicarboximide) pigments. Acta Crystallogr B 1989;45:69–77.
[76] Mizuguchi JN. N'-Bis(2-phenethyl)perylene-3,4:9,10-bis(dicarboximide). Acta Crystallogr C 1998;54:1479–81.
[77] Nather C, Bock H, Havlas Z, Hauck T. Solvent-shared and solvent-separated ion multiples of perylene radical anions and dianions: an exemplary case of alkali metal cation solvation. Organomet 1998;17(21):4707–15.
[78] Calzaferri G, Imhof R, Törnroos KW. Structural and vibrational properties of the octanuclear silasesquioxane $C_6H_{13}(H_7Si_8O_{12})$. J Chem Soc Dalton Trans; 1994:3123–8.
[79] Bassindale AR, Chen H, Liu Z, MacKinnon IA, Parker DJ, Taylor PG, et al. A higher yielding route to octasilsesquioxane cages using tetrabutylammonium fluoride, part 2: further synthetic advances, mechanistic investigations and X-ray crystal structure studies into the factors that determine cage geometry in the solid state. J Organomet Chem 2004;689:3287–300.
[80] Dittmar U, Hendan BJ, Florke U, Heinrich C, Marsmann C. Funktionalisierte Octa-(propylsilsesquioxane) $(3\text{-}XC_3H_6)_8(Si_8O_{12})$ Modellverbindungen fiir oberfl ichenmodifizierte Kieselgele. J Organomet Chem 1995;489:185–94.
[81] Lucke S, Stoppeck-Langner K, Krebs B, Lage M. Syntheses and structures of delta-halopropyl-octa(silsesquioxanes). Z Anorg Allg Chem 1997;623:1243–6.